ChemistryOPEN

Supporting Information

Anion Binding Properties of Alkynylplatinum(II) Complexes with Amide-Functionalized Terpyridine: Host–Guest Interactions and Fluoride Ion-Induced Deprotonation**

Margaret Ching-Lam Yeung, Ben Wai-Kin Chu, and Vivian Wing-Wah Yam*[a]

open_201402019_sm_miscellaneous_information.pdf

Materials and reagents: 2,2′:6′,2″-Terpyridine-3′,5′-dicarboxylic acid was synthesized according to the literature procedure.[1] Tetra-*n*-butylammonium hexafluorophosphate was purchased from Apollo Scientific Ltd. and was recrystallized for three times from hot absolute ethanol and then dried under vacuum for 12 hours before use. Acetonitrile (99 + %, for spectroscopy) was purchased from Acros. Acetone (ACS spectrophotometric grade, ≥ 99.5 %) was purchased from Aldrich. All other reagents were of analytical grade and were used as received.

Syntheses of terpyridine ligands

2,2′:6′,2″-Terpyridine-3′,5′-dicarboxylic acid phenylamide [tpy–(CONHPh)$_2$]: To 2,2′:6′,2″-terpyridine-3′,5′-dicarboxylic acid (500 mg, 1.55 mmol) was added $SOCl_2$ (10 ml) and the resultant mixture was refluxed overnight with a $CaCl_2$ drying tube equipped at the opening of the condenser. The $SOCl_2$ was then removed by distillation and to the solid was added dry dichloromethane (20 ml) to give a yellow suspension. To this mixture was added dropwise a solution containing dry dichloromethane (20 ml), aniline (0.29 ml, 3.20 mmol) and dry triethylamine (0.5 ml) over 30 minutes at 0 ^{o}C and the mixture was then stirred overnight at room temperature. The resulting mixture was washed with saturated aqueous $NaHCO_3$ solution and dried over anhydrous $MgSO_4$. After removal of solvent, recrystallization of the residue from dichloromethane-ethanol gave the pure product as a white solid. Yield: 320 mg (44 %).^{1}H NMR (400 MHz, $CDCl_3$, 298 K, δ/ppm): δ 7.00-7.03 (t, *J* = 7.3 Hz, 2H, –$C_6\boldsymbol{H_5}$NH–), 7.15-7.18 (m, 6H, –$C_6\boldsymbol{H_5}$NH–), 7.52-7.56 (dt, *J* = 1.4, 7.7 Hz, 2H, terpyridyl H), 7.61-7.63 (d, *J* = 7.7 Hz, 4H, terpyridyl H), 7.73 (s, 1H, terpyridyl H), 7.86-7.88 (d, *J* = 7.7 Hz, 2H, terpyridyl H), 8.10 (br s, 2H, –$C_6\boldsymbol{H_5}$NH–), 11.30 (br s, 2H, –$C_6H_5N\boldsymbol{H}$–); positive-ion FAB-MS, *m/z*: 472 $[M + H]^+$; elemental analysis calcd (%) for $C_{29}H_{21}N_5O_2$•EtOH: C 71.93, H 5.26, N 13.53; found: C 71.63, H 5.23, N 13.32.

2,2′:6′,2″-Terpyridine-3′,5′-dicarboxylic acid hexylamide [tpy–(CONHC$_6$H$_{13}$)$_2$]: The procedure was similar to the preparation of tpy–(CONHPh)$_2$ except that *n*-hexylamine (0.42 ml, 3.20 mmol) was used in place of aniline to give the pure product as a white solid. Yield: 357 mg (47 %). ^{1}H NMR (400 MHz, $CDCl_3$, 298 K, δ/ppm): δ 0.87-0.92 (t, *J* = 6.8 Hz, 6H, –CH_3), 1.30-1.34 (m, 12H, –CH_2–), 1.48-1.52 (m, 4H, –CH_2–), 3.35-3.41 (q, *J* = 7.0 Hz, 4H, –NHC$\boldsymbol{H_2}$–), 7.22

(br s, 2H, –CONH–), 7.32-7.37 (ddd, *J* = 1.4, 4.7, 7.7 Hz, 2H, terpyridyl H), 7.80-7.85 (dt, *J* = 1.4, 7.7 Hz, 2H, terpyridyl H), 8.04-8.06 (d, *J* = 7.7 Hz, 2H, terpyridyl H), 8.15 (s, 1H, terpyridyl H), 8.55-8.56 (d, *J* = 4.7 Hz, 2H, terpyridyl H); positive-ion FAB-MS, *m/z*: 488 $[M + H]^+$; elemental analysis calcd (%) for $C_{29}H_{37}N_5O_2$•0.5MeOH: C 70.35, H 7.80, N 13.91; found: C 70.46, H 7.62, N 14.00.

Syntheses of chloroplatinum(II) terpyridine complexes

[Pt{tpy–(CONHPh)$_2$}Cl]OTf: This was synthesized by the modification of the literature procedure for the synthesis of [Pt(tpy)Cl]OTf[2–5] using tpy–(CONHPh)$_2$ (150 mg, 0.32 mmol) in place of 2,2′:6′,2″-terpyridine. Subsequent recrystallization by diffusion of diethyl ether vapor into the acetonitrile solution of this precursor complex gave the pure product as a yellow solid. Yield: 220 mg (80 %).^{1}H NMR (400 MHz, CD_3CN, 298 K, δ/ppm): δ 7.27-7.31 (t, *J* = 7.6 Hz, 2H, $–C_6\boldsymbol{H_5}NH–$), 7.45-7.49 (t, *J* = 7.6 Hz, 4H, $–C_6\boldsymbol{H_5}NH–$), 7.74-7.76 (d, *J* = 7.6 Hz, 4H, $–C_6\boldsymbol{H_5}NH–$), 7.85-7.89 (dt, *J* = 1.7, 7.4 Hz, 2H, terpyridyl H), 8.25-8.33 (m, 4H, terpyridyl H), 8.76 (s, 1H, terpyridyl H), 9.19-9.20 (d, *J* = 5.4 Hz, 2H, terpyridyl H), 9.54 (br s, 2H, $–C_6H_5N\boldsymbol{H}–$); IR (Nujol, ν/cm^{-1}): 1682 (m) ν(C=O), 1157 (s) ν(S=O); positive-ion FAB-MS, *m/z*: 702 $[M – OTf]^+$; elemental analysis calcd (%) for $C_{30}H_{21}ClF_3N_5O_5PtS$•$H_2O$: C 41.46, H 2.67, N 8.06; found: C 41.47, H 2.62, N 8.10.

[Pt{tpy–(CONHC$_6$H$_{13}$)$_2$}Cl]OTf: The procedure was similar to that for the preparation of [Pt{tpy–(CONHPh)$_2$}Cl]OTf except that tpy–(CONHC$_6$H$_{13}$)$_2$ (156 mg, 0.32 mmol) was used in place of tpy–(CONHPh)$_2$ and subsequent recrystallization by diffusion of diethyl ether vapor into the dichloromethane solution of this precursor complex gave the pure product as an orange solid. Yield: 241 mg (87 %). ^{1}H NMR (400 MHz, CD_3CN, 298 K, δ/ppm): δ 0.90-0.93 (t, *J* = 7.0 Hz, 6H, $–CH_3$), 1.33-1.43 (m, 12H, $–CH_2–$), 1.62-1.69 (m, 4H, $–CH_2–$), 3.46-3.50 (q, *J* = 7.0 Hz, 4 H, $–NHC\boldsymbol{H_2}–$), 7.61 (br s, 2H, –CONH–), 7.82-7.86 (ddd, *J* = 1.4, 5.6, 7.8 Hz, 2H, terpyridyl H), 8.15-8.17 (d, *J* = 7.8 Hz, 2H, terpyridyl H), 8.27 (s, 1H, terpyridyl H), 8.27-8.33 (dt, *J* = 1.4, 7.8 Hz, 2H, terpyridyl H), 9.11-9.13 (d, *J* = 5.6 Hz, 2H, terpyridyl H); IR (Nujol, ν/cm^{-1}): 1659 (m) ν(C=O), 1157 (s) ν(S=O); positive-ion FAB-MS, *m/z*: 718 $[M – OTf]^+$; elemental analysis calcd (%) for $C_{30}H_{37}ClF_3N_5O_5PtS$•1.5$CH_2Cl_2$: C 38.03, H 4.05, N 7.04; found: C 38.27, H 4.07, N 7.02.

Syntheses of alkynylplatinum(II) terpyridine complexes

[Pt{tpy–(CONHPh)$_2$}(C≡CPh)]PF$_6$ (1): This was synthesized according to the modification of a method previously reported for the alkynylplatinum(II) terpyridine complexes[6] except that [Pt{tpy–(CONHPh)$_2$}Cl]OTf (200 mg, 0.23 mmol) and phenylacetylene (71 mg, 70 mmol) were used to give **1** as an orange solid. Yield: 131 mg (61 %). ^{1}H NMR (400 MHz, CD_3CN, 298 K, δ/ppm): δ 7.27-7.32 (m, 3H, $-C{\equiv}CC_6\boldsymbol{H_5}$), 7.35-7.39 (t, J = 7.6 Hz, 2H, $-C_6\boldsymbol{H_5}NH-$), 7.45-7.49 (t, J = 7.6 Hz, 4H, $-C_6\boldsymbol{H_5}NH-$), 7.53-7.59 (m, 2H, $-C{\equiv}CC_6\boldsymbol{H_5}$), 7.74-7.76 (d, J = 7.6 Hz, 4H, $-C_6\boldsymbol{H_5}NH-$), 7.82-7.85 (dt, J = 1.4, 7.3 Hz, 2H, terpyridyl H), 8.28-8.32 (m, 4H, terpyridyl H), 8.71 (s, 1H, terpyridyl H), 9.44 (br s, 2H, $-C_6H_5N\boldsymbol{H}-$), 9.46-9.47 (d, J = 5.2 Hz, 2H, terpyridyl H); IR (Nujol, ν/cm^{-1}): 2122 (w) ν(C≡C), 1682 (m) ν(C=O), 849 (s) ν(P–F); positive-ion FAB-MS, *m/z*: 767 $[M - PF_6]^+$; elemental analysis calcd (%) for $C_{37}H_{26}F_6N_5O_2PPt$: C 48.69, H 2.87, N 7.67; found: C 48.63, H 2.91, N 7.90.

[Pt{tpy–(CONHC$_6$H$_{13}$)$_2$}(C≡CPh)]PF$_6$ (2): The procedure was similar to that for the preparation of **1** except that [Pt{tpy–(CONHC$_6$H$_{13}$)$_2$}Cl]OTf (200 mg, 0.23 mmol) was used in place of [Pt{tpy–(CONHPh)$_2$}Cl]OTf to give **2** as a dark red solid. Yield: 120 mg (56 %). ^{1}H NMR (400 MHz, CD_3CN, 298 K, δ/ppm): δ 0.90-0.94 (t, J = 7.0 Hz, 6H, $-CH_3$), 1.34-1.43 (m, 12H, $-CH_2-$), 1.62-1.69 (m, 4H, $-CH_2-$), 3.46-3.50 (q, J = 6.6 Hz, 4H, $-NHC\boldsymbol{H_2}-$), 7.29-7.39 (m, 3H, $-C_6H_5-$), 7.50-7.53 (br s, 2H, –CONH–), 7.53-7.56 (m, 2H, $-C_6H_5-$), 7.79-7.83 (ddd, J = 1.3, 5.4, 7.8 Hz, 2H, terpyridyl H), 8.15-8.17 (d, J = 7.8 Hz, 2H, terpyridyl H), 8.22 (s, 1H, terpyridyl H), 8.28-8.32 (dt, J = 1.3, 7.8 Hz, 2H, terpyridyl H), 9.40-9.41 (d, J = 5.4 Hz, 2H, terpyridyl H); IR (Nujol, ν/cm^{-1}): 2121 (w) ν(C≡C), 1659 (m) ν(C=O), 841 (s) ν(P–F); positive-ion FAB-MS, *m/z*: 783 $[M - PF_6]^+$; elemental analysis calcd (%) for $C_{37}H_{42}F_6N_5O_2PPt{\bullet}MeOH$: C 47.50, H 4.82, N 7.28; found: C 47.32, H 4.53, N 7.27.

Physical measurements and instrumentation: ^{1}H NMR spectra were recorded on a Bruker AVANCE 400 (400 MHz) Fourier transform NMR spectrometer at ambient temperature with tetramethylsilane (Me_4Si) as an internal reference. Positive-ion fast atom bombardment (FAB) mass spectra were recorded on a Thermo Scientific DFS High Resolution Magnetic Sector mass spectrometer. Electrospray-ionization (ESI) mass spectra were obtained on a Finnigan LCQ mass spectrometer. Infrared (IR) spectra were recorded on a Bio-Rad FTS-7 Fourier transform infrared spectrophotometer (4000–400 cm^{-1}). Elemental analyses were performed on a Flash EA 1112 elemental analyzer at the Institute of Chemistry of the Chinese Academy of Sciences, Beijing. UV-Vis absorption spectra were recorded on a Cary 50 (Varian) spectrophotometer equipped with a Xenon flash lamp. Steady state excitation and emission spectra were recorded using a Spex Fluorolog-3 Model FL3-211 fluorescence spectrofluorometer equipped with a R2658P PMT detector. All the emission spectra were corrected for PMT response. Emission lifetime measurements were performed using a conventional laser system. The excitation source used was a 355-nm output (third harmonic) of a Spectra-Physics Quanta-Ray Q-switched GCR-150-10 pulsed Nd-YAG laser. Luminescence decay signals were detected by a Hamamatsu R928 PMT and recorded on a Tektronix Model TDS-620A (500MHz, 2 GS/s) digital oscilloscope. The luminescence decay traces were analyzed using a program for single exponential fits. All solutions for emission lifetime studies were degassed on a high-vacuum line in a two-compartment cell consisting of a 10-ml Pyrex bulb and a 1-cm path length quartz cuvette and sealed from the atmosphere by a Bibby Rotaflo HP6 Teflon stopper. The solutions were rigorously degassed with at least four successive freeze-pump-thaw cycles.

Binding constant determination: Supporting electrolyte (0.1 M ^{n}Bu$_4$NPF$_6$) was added to maintain the ionic strength of the sample solution constant during the titration to avoid any changes in the ionic strength of the medium. The binding constants, K_s, of 1:1 host-guest complexation system were determined by a nonlinear least-squares fit[7] of the emission intensities (I) against the concentration of guest added (C_G) according to Equation (1):

$$I = I_0 + \frac{I_{\text{lim}} - I_0}{2C_0}\ [C_0 + C_G + 1/K_s - [(C_0 + C_G + 1/K_s)^2 - 4C_0C_G]^{1/2}\ ] \tag{1}$$

where I_0 and I are the emission intensities of the host at the wavelength of interest in the absence and presence of the guest, respectively; C_0 is the concentration of host; I_{lim} is the limiting value of the emission intensity in the presence of excess amount of guest.

References:

[1] F. H. Case, W. A. Butte, *J. Org. Chem.* **1961**, *26*, 4415 – 4418.

[2] J. A. Bailey, M. G. Hill, R. E. Marsh, V. M. Miskowski, W. P. Schaefer, H. B. Gray, *Inorg. Chem.* **1995**, *34*, 4591 – 4599.

[3] S. D. Cummings, R. Eisenberg, *Inorg. Chem.* **1995**, *34*, 2007 – 2014.

[4] R. Büchner, J. S. Field, R. J. Haines, C. T. Cunningham, D. R. McMillin, *Inorg. Chem.* **1997**, *36*, 3952 – 3956.

[5] M. Howe-Grant, S. J. Lippard, *Inorg. Synth.* **1980**, *20*, 101 – 105.

[6] V. W. W. Yam, R. P. L. Tang, K. M. C. Wong, K. K. Cheung, *Organometallics* **2001**, *20*, 4476 – 4482.

[7] J. Bourson, J. Pouget, B. Valeur, *J. Phys. Chem.* **1993**, *97*, 4552 – 4557.

Table S1 Photophysical data for complexes **1** and **2**.

Complex	**Medium** (***T*** **/ K**)	**Absorption** λ_{abs} **/ nm** (ε **/ dm**^{3} **mol**$^{-1}$ **cm**$^{-1}$)	**Emission** λ_{em} **/ nm** (τ **/ μs**)
1	CH_3CN (298)	250 (56000), 297 (24890), 317 sh (18080), 330 sh (15870), 344 sh (14420), 445 (4050)	662 (0.14)
2	CH_3CN (298)	251 (42830), 286 sh (25140), 298 (25340), 318 sh (14380), 332 sh (13180), 347 (13060), 444 (4420)	653 (0.20)
	Acetone (298)	349 (11200), 445 (3730)	652 (0.24)

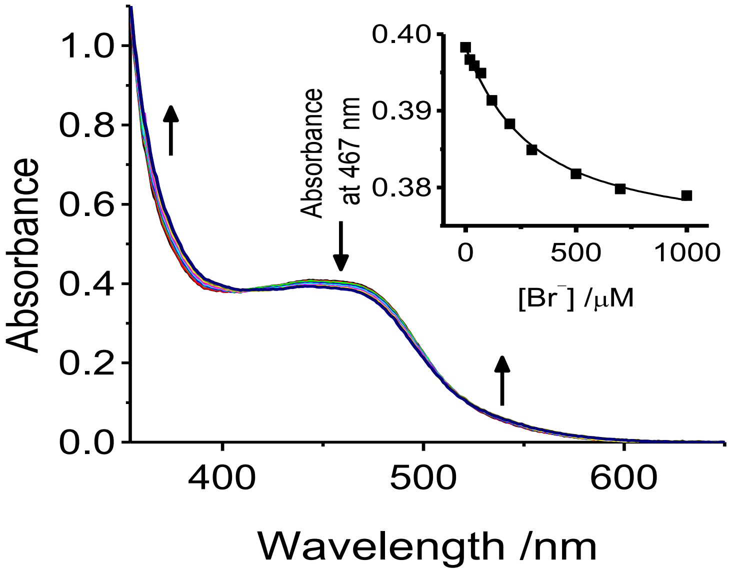

Figure S1 UV-Vis absorption spectral changes of **1** (100 μM) in acetonitrile (0.1 M ^{n}Bu$_4$NPF$_6$) upon addition of ^{n}Bu$_4$NBr. Inset: plot of absorbance at 467 nm against various concentrations of Br$^-$ ion.

Table S2 Emission lifetimes of **1** and **2** (100 μM) in the absence and in the presence of various anions (750 μM).

Complex	**Anion**	**τ / μs**
1[a]	None	0.12
	Cl^-	< 0.05
	Br^-	< 0.05
2[b]	None	0.20
	F^-	–[c]
	Cl^-	< 0.05
	Br^-	0.06
	I^-	0.07
	AcO^-	< 0.05

[a] Measured in degassed acetonitrile (0.1 M ^{n}Bu$_4$NPF$_6$).

[b] Measured in degassed acetone (0.1 M ^{n}Bu$_4$NPF$_6$).

[c] Precipitations occurred upon degassing.

Table S3 Binding constants (log K_s) and detection limits of **1** and **2** for various anions.

		Log K_s		Detection Limit /μM
Complex	**Anion**	**UV-Vis**	**Emission**	
1[a]	F^-	–[c]	–[c]	–[e]
	Cl^-	–[d]	4.46 ± 0.05	9.86
	Br^-	–[d]	3.69 ± 0.05	18.35
	I^-	–[d]	–[d]	–[e]
	AcO^-	–[c]	–[c]	–[e]
	$H_2PO_4^-$	–[c]	–[c]	–[e]
2[b]	F^-	–[e]	4.15 ± 0.04	7.72
	Cl^-	4.03 ± 0.04	4.08 ± 0.01	12.67
	Br^-	–[d]	3.64 ± 0.01	16.96
	I^-	–[d]	3.41 ± 0.01	23.09
	AcO^-	4.40 ± 0.04	4.40 ± 0.08	5.75
	$H_2PO_4^-$	–[c]	–[c]	–[e]

[a] Measured in acetonitrile (0.1 M $^n Bu_4NPF_6$).
[b] Measured in acetone (0.1 M $^n Bu_4NPF_6$).
[c] Precipitations occurred upon anion addition.
[d] Spectral changes were too small for accurate determination of log K_s.
[e] Not determined.

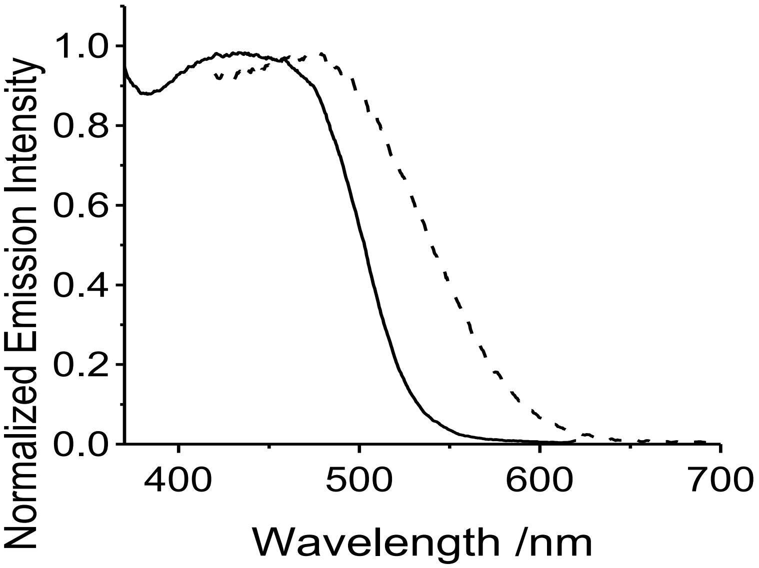

Figure S2 Excitation spectra of **2** (100 μM) in acetone (0.1 M $^{n}Bu_4NPF_6$) in the absence (solid line) and in the presence of F^- ion (7 equiv.) (dashed line), monitored at 653 and 750 nm, respectively.

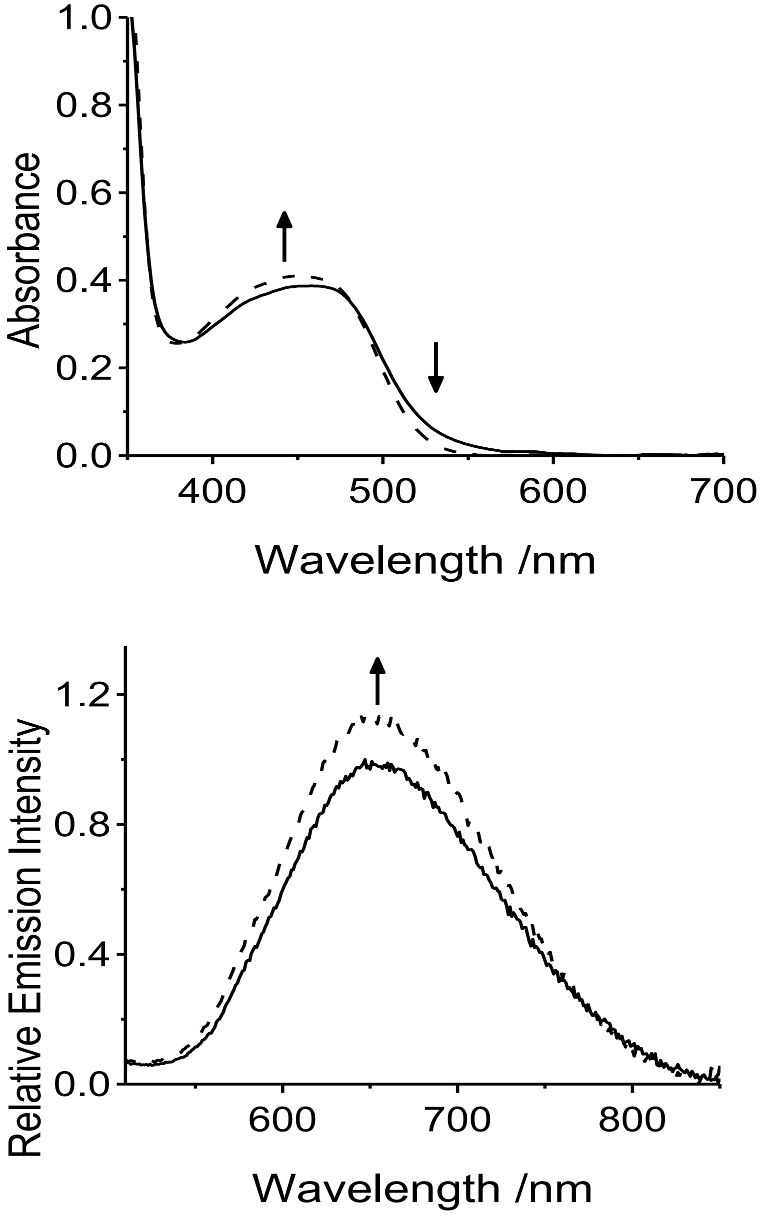

Figure S3 (Top) UV-Vis absorption and (bottom) emission spectral changes of **2** (100 μM) (solid line) in acetone (0.1 M $^{n}Bu_4NPF_6$) in the presence of trifluoroacetic acid (4 equiv.) (dashed line).

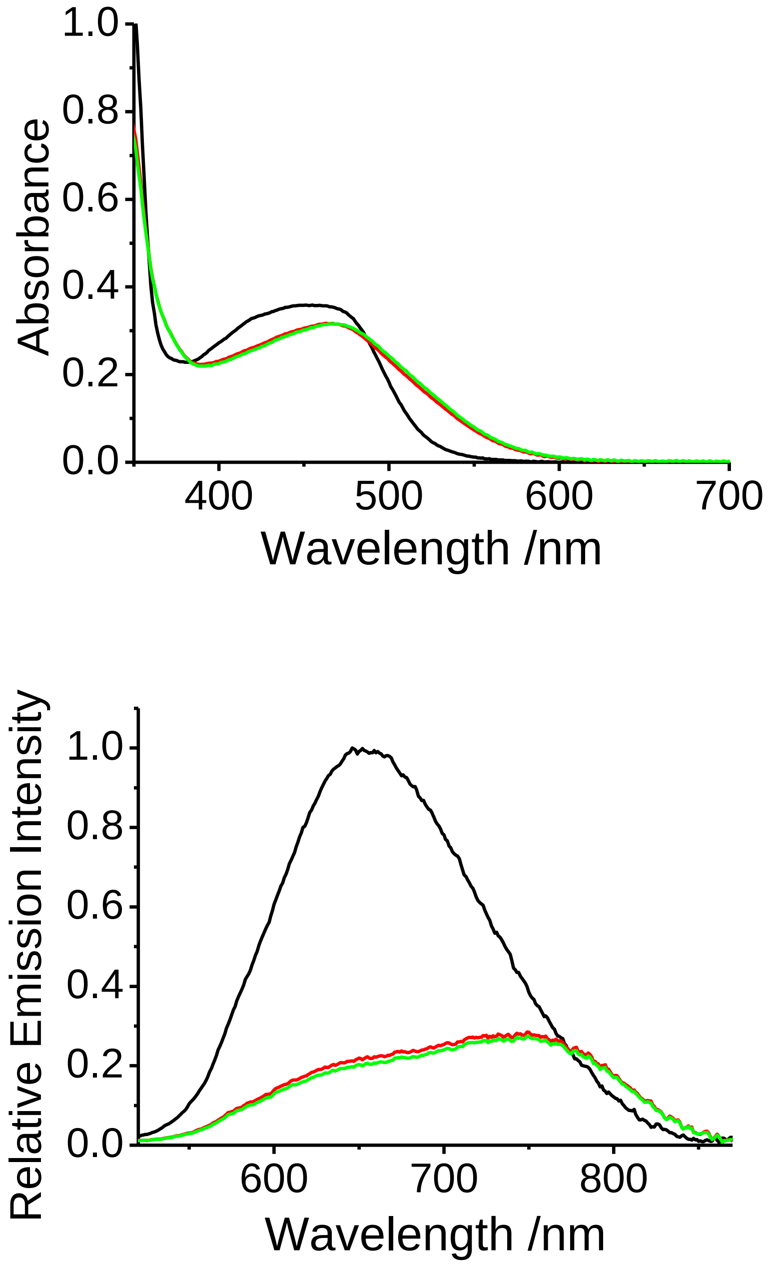

Figure S4 (Top) UV-Vis absorption and (bottom) emission spectral changes of **2** (100 μM) (black line) in acetone (0.1 M $^{n}Bu_4NPF_6$) in the presence of $^{n}Bu_4NF$ (4 equiv.) (red line), and in the mixture in the presence of CF_3COONa (4 equiv.) (green line).

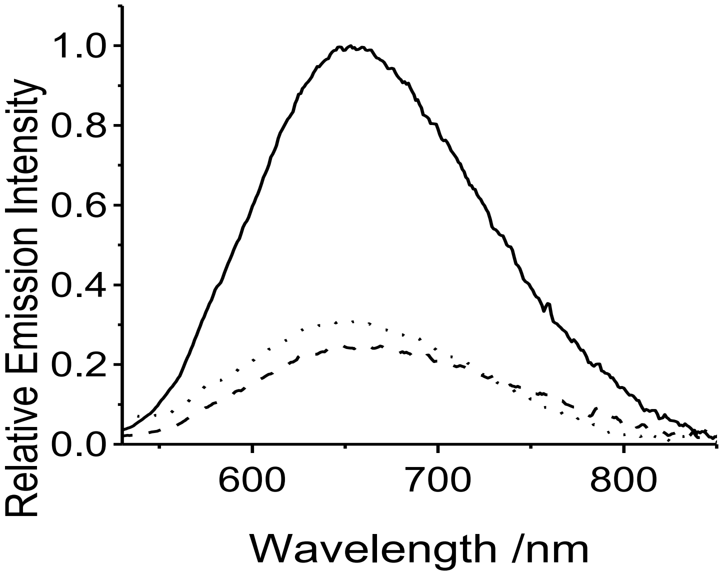

Figure S5 Emission spectral changes of **2** (100 μM) (solid line) in acetone (0.1 M $^{n}Bu_4NPF_6$) in the presence of $^{n}Bu_4NCl$ (5 equiv.) (dashed line), and in the mixture in the presence of trifluoroacetic acid (5 equiv.) (dotted line).

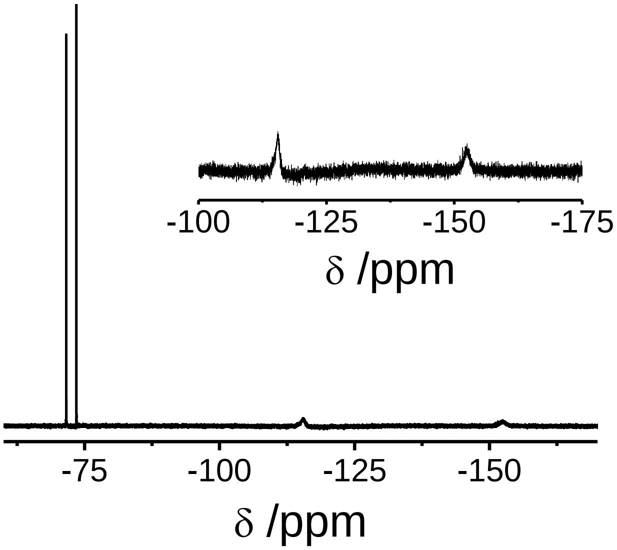

Figure S6 ^{19}F NMR spectrum and the expanded region from δ –100 ppm to δ –175 ppm of **2** in the presence of an excess of $^{n}Bu_4NF$ in D^6-acetone.

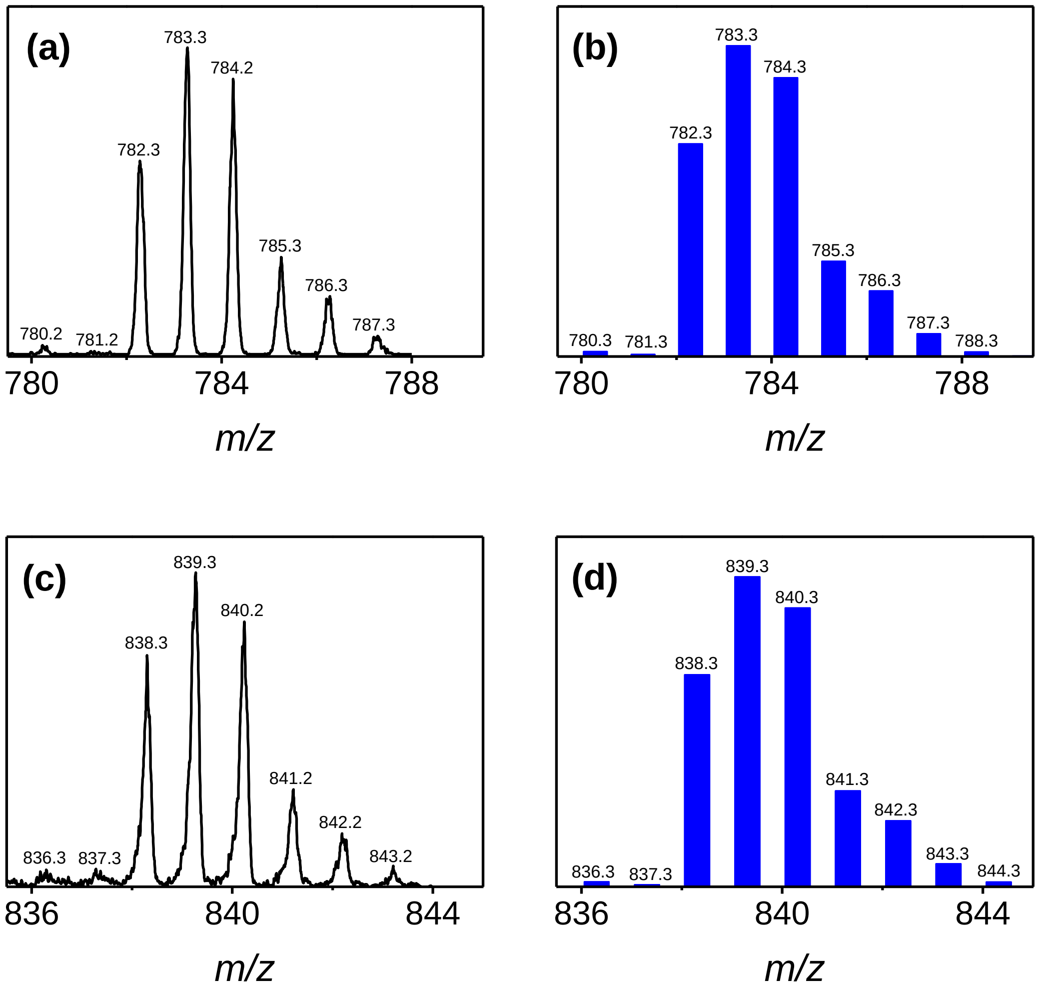

Figure S7 (a) Expanded ion cluster at *m/z* 783 from positive ESI-mass spectrum, prepared in acetone, and (b) simulated isotope pattern for **2**, $[M - PF_6]^+$. (c) Expanded ion cluster at *m/z* 839 from negative ESI-mass spectrum and (d) simulated isotope pattern for the ion-bound adduct of **2** in acetone in the presence of F^- ion (6 equiv.), $[M - PF_6 + 2F + H_2O]^-$.

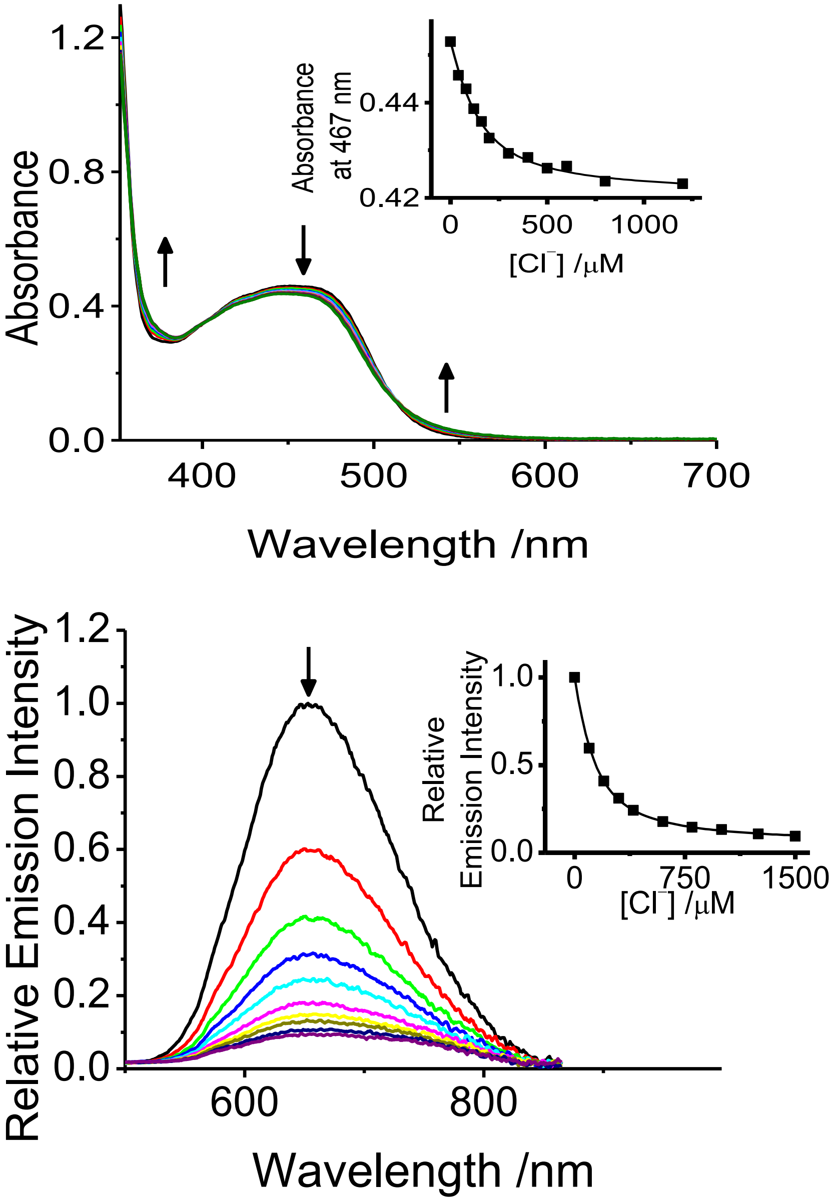

Figure S8 (Top) UV-Vis absorption and (bottom) emission spectral changes of **2** (100 μM) in acetone (0.1 M $^{n}Bu_4NPF_6$) upon addition of $^{n}Bu_4NCl$. Insets: plot of absorbance at 467 nm and relative emission intensity at 653 nm against various concentrations of Cl^- ion and their theoretical fit for 1:1 binding stoichiometry.

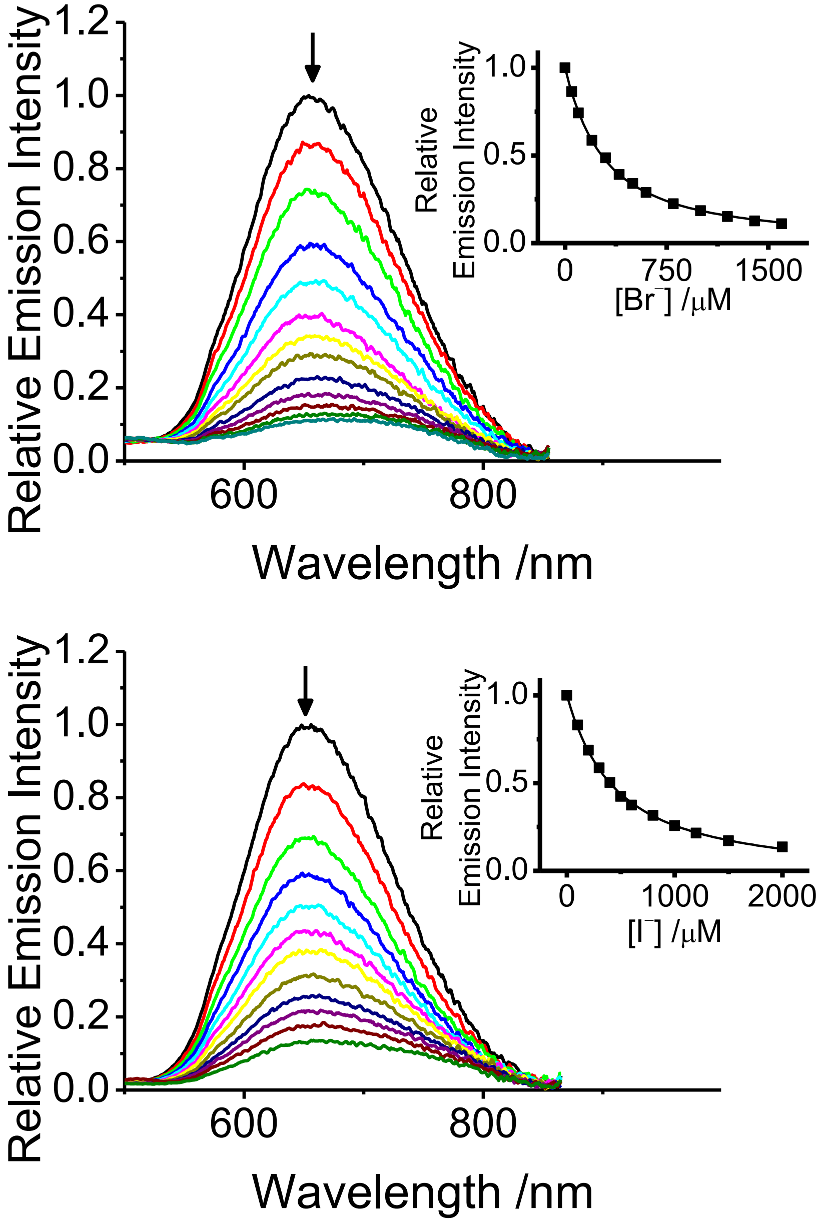

Figure S9 Emission spectral changes of **2** (100 μM) in acetone (0.1 M ^{n}Bu$_4$NPF$_6$) upon addition of (top) ^{n}Bu$_4$NBr and (bottom) ^{n}Bu$_4$NI. Insets: plot of relative emission intensity at 653 nm against various concentrations of Br$^-$ and I$^-$ ions and their theoretical fit for 1:1 binding stoichiometry.